Core exciton, valence exciton, and optical properties of yttrium aluminum garnet ($Y_3Al_5O_{12}$)

Yong-Nian Xu, Yu Chen, Shang-Di Mo, and W. Y. Ching*
Department of Physics, University of Missouri-Kansas City, Kansas City, Missouri 64110
(Received 20 February 2002; revised manuscript received 10 April 2002; published 28 May 2002)

The electronic transitions from deep core levels, semicore levels, and valence bands to the empty conduction bands in yttrium aluminum garnet ($Y_3Al_5O_{12}$) (YAG) are studied by first-principles calculations that explicitly take into account the excitonic effect. The electron energy-loss near edge structure and the valence-band optical properties thus obtained are in very good agreement with the measured optical data. The electron-hole interaction in YAG is found to be much weaker for valence-band optical transitions than for core transitions.

DOI: 10.1103/PhysRevB.65.235105 PACS number(s): 71.35.Cc, 78.55.Hx

Yttrium aluminum garnet ($Y_3Al_5O_{12}$), or YAG, is one of the most important optical materials with a wide range of applications such as laser host material, optical lens, and thermal barrier coating.[1,2] This is primarily attributed to its outstanding mechanical stability, low thermal expansion and conductivity, low acoustic losses, and excellent optical properties. YAG has a cubic garnet structure (space group $Ia3d$ or O_h^{10}) consisting of interconnected and slightly distorted octahedrons, tetrahedrons, and dodecahedrons with shared O atoms at the corner.[3] The Y ion at the 24(c) position is dodecahedrally coordinated to eight O ions, which occupy the 96(h) sites. There are two Al sites, the octahedrally coordinated Al_{oct} at the 16(a) site and the tetrrahedrally coordinated Al_{tet} at the 24(d) site. Different cation environments and the cubic structure are the basis of many of its electro-optical and electroceramic applications.[1,2] Because of its complex crystal structure, the electronic structure of YAG has only been studied recently.[4] The band structure is that of a typical ionic oxide with mixed ionic and covalent bonding. The optical properties of YAG have never been seriously calculated in spite of a considerable amount of experimental data.[5–7]

YAG is also a very valuable component in high-temperature ceramic composites because of its well-known resistance to creep.[8–10] At the internal grain boundaries (GB) in sapphire and other oxides, YAG is frequently seen as the precipitated phase due to the propensity of Y segregating to GB or the interfacial region.[11] The mechanism of Y segregation and the structure at the oxide GB is one of the most outstanding problems in materials science. Structural characterization is a key step in the understanding of these phenomena. In recent years, electron energy-loss spectroscopy, in conjunction with dedicated scanning transmission electron microscopy, has emerged as a powerful tool for studying the electronic structure of a crystal and its microstructures. In particular, the electron energy-loss near edge structure (EELNES) contains detailed information on the local chemical and structural environment of the atom undergoing an inner-shell excitation.[12] The EELNES spectra of YAG have been measured[13] and shown to be very different from the component oxides α-Al_2O_3 and Y_2O_3. The EELNES is especially useful in characterizing the complex ceramic structures such as GB with segregated ions.

In this paper, we present a detailed study of the EELNES spectra and the VB optical transitions. By including the excitonic effect in both cases, very good agreement with the experimental data is achieved. We also demonstrate the different nature of the excitonic effects from the deep core and those from the VB.

It has long been recognized that the core exciton plays a crucial role in defining the EELNES spectra of materials.[12] Popular approaches to treat the core-hole effect include the Slater transition method or using the $Z+1$ approximation.[14,15] Depending on the actual implementation, consistent agreement with measured spectra has seldom been achieved by these methods. The Coulomb interaction between the excited electron in the conduction band (CB) and the hole left in the core can strongly modify the unoccupied states. On the other hand, the valence-band (VB) optical properties of insulators within the framework of the random-phase approximation are generally interpreted in terms of interband transitions from the VB to the CB.[16] It is generally assumed that electron-hole interactions in the VB optical properties can be neglected. However, the presence of strong excitonic peaks in the VB optical properties of many oxides, such as α-Al_2O_3,[17,18] MgO, $MgAl_2O_4$,[18] Y_2O_3,[19] and α-SiO_2,[20] is well known.

Our calculation starts with the ground-state electronic structure of YAG using a density-functional-theory-based method presented elsewhere.[4] In the present spectral calculation, additional orbitals (Y $7s$, $6p$, $6d$; Al $5s$, $5p$, $4d$, and O $4s$) were added to the basis set (referred to as the extended basis) to ensure sufficient accuracy for transitions of up to 35 eV in the CB. The semicore Y $4p$ states were treated as the VB states. For the EELNES calculation, we used the recently developed ''supercell'' method,[21] which explicitly includes the electron core-hole interaction. The unit cell of YAG ($a = 12.000$ Å, 80 atoms in the primitive cell) is sufficiently large to effectively serve as a supercell. In this method, the initial ground state and the final core-hole states are calculated separately. The final states involve the excitation of a core electron from a specific atom to the lowest CB, leaving behind a hole in the core of that atom. This is implemented by specific instructions in the program for constrained occupation of the orbital states, which are summed up to obtain the total crystal charge density at each iteration. The interaction and the associated screening effect between the electron-hole pair are fully accounted for by the self-consistent iterations of the Kohn-Sham equation in the final state calculation. The EELNES intensity function is calculated according to[9]

 ©2002 The American Physical Society

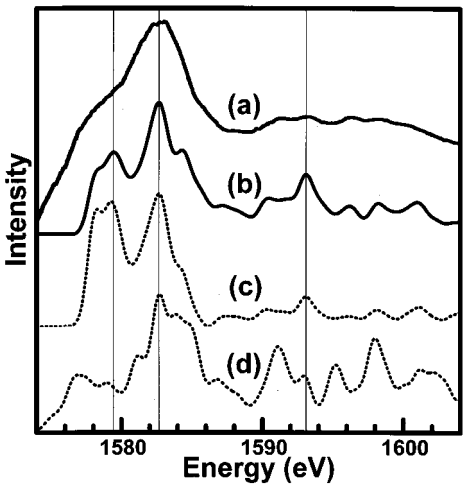

FIG. 1. Comparison of the measured (Ref. 13) (a) and calculated (b) Al *K* edge in YAG. The calculated spectrum is the weighted sum of the contributions from Al at the tetrahedral site and Al at the octahedral site. The energy scale is set by matching the transition energy with the edge onset. The LDOS (Al-p) from the ground-state calculation (c) and the final-state calculation (d) are each shifted to align with the experimental peak. They are the weighted sums of the LDOS at Al_{oct} and Al_{tet}.

$$I(\hbar\omega) \propto \frac{e^2}{m\pi\hbar\omega^2} \sum_f |\langle f|\vec{\mathbf{P}}|i\rangle|^2 \delta(\hbar\omega - E_f + E_i),$$

where E_i and E_f are the orbital energies of the initial and final states, respectively. $\mathbf{P} = -i\nabla$ is the momentum operator and $\hbar\omega$ is the transition energy. The inclusion of the matrix elements ensures that the dipole selection rule is automatically satisfied.

A special advantage of the present method is that the onset energy of the EELNES edge or the transition energy can be obtained from the difference in the total energies (TE) for the initial- and final-state calculations. In the past analysis of EELNES data, a common practice is to use the symmetry-projected local density of states (LDOS) of the CB from the ground-state calculation. In the constant matrix approximation and neglecting any electron-hole interaction, the *K* edges of Al and O can be represented by the p component of the Al and O LDOS, respectively, and the Al *L* edge can be interpreted by the $(s+d)$ components of the Al LDOS. The spectrum is usually shifted to align the main peak in the CB LDOS with the measured spectrum with no reference to the actual energy scale. One is contented with the presence (or the absence) of certain peaks with little attention to the relatively intensities. Another special feature of the present method is that in each calculation, a specific atom in the supercell is excited. Hence, the difference between the spectra from Al_{tet} and Al_{oct} in YAG, which has slightly different transition energies, can be delineated. Experimental measurement gives the combined spectra from both sites.

The calculated Al *K* ($1s \rightarrow$CB), Al $L_{2,3}$ ($2p \rightarrow$CB), and O *K* ($1s \rightarrow$CB) edges in YAG are shown in Figs. 1, 2, and 3, respectively. Also displayed are the experimental data from

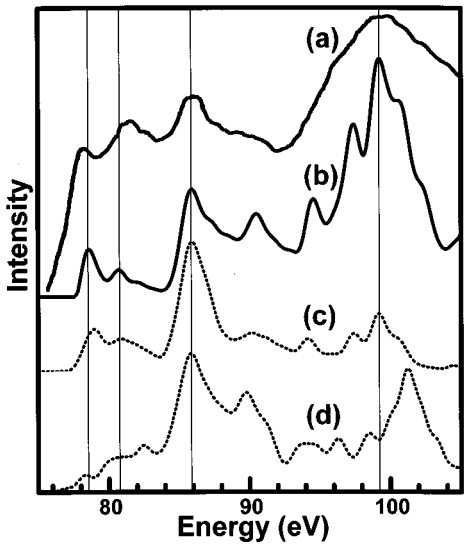

FIG. 2. Same as for Fig. 1 but for the Al $L_{2,3}$ edge. The LDOS is the $(s+d)$ component of Al.

Gülgün *et al.*[13] Additional test calculations using a 160-atom cubic cell show no discernable difference. For consistency, all calculated spectra were broadened by a Gaussian of 1.0 eV (full width at half maximum). We prefer not to use the broadening factor as a means to improve the agreement with the experimental spectra. For the Al *K* and Al $L_{2,3}$ edges, the calculated spectra are the weighted sums of the contributions from Al_{oct} and Al_{tet}. Also displayed in Figs. 1–3 are the LDOS from both the ground-state and final-state calculations. For the Al LDOS, the spectra are the weighted sum of the site-projected LDOS from Al_{oct} and Al_{tet}. In both cases, the LDOS spectra are shifted to produce the best agreement with the measured spectrum. As can be seen, the ground-state LDOS interpretation is totally unsatisfactory. The LDOS from the final-state calculation, which includes the

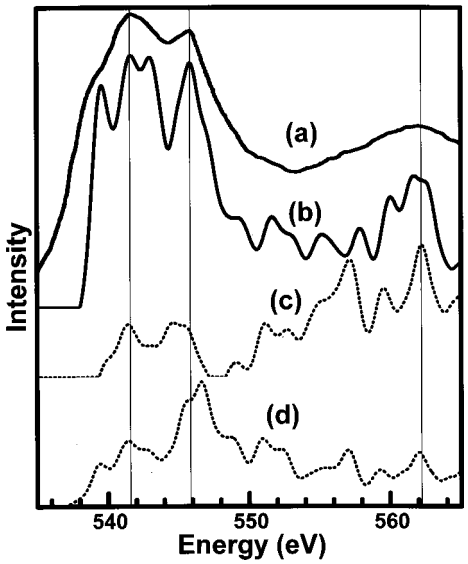

FIG. 3. Comparison of the calculated and measured O *K* edge in YAG crystal. The notations are the same as Fig. 1.

core-hole effect, gives a marked improvement. However, they are still not as good as the actual calculation, especially in the relative intensities of various peaks. All the major structures in the measured curves are reproduced by our calculation. For the Al $L_{2,3}$ edge, the edge onset is controlled mainly by Al_{oct}, because it has a slightly lower transition energy. For the Al edges, a combined sum of contributions from the two different sites is required to produce a satisfactory agreement. Since the energy resolution in the experimental spectra is rather low, the theoretical curve can resolve the buried structures as is quite evident in the case of the O *K* edge. It should also be pointed out that the Al *K* and Al $L_{2,3}$ edges from the Al_{oct} site in YAG differ substantially from those of α-Al_2O_3,[21] even though Al in α-Al_2O_3 is also octahedrally coordinated. Therefore, one cannot use the simple concept of the coordinating shell to interpret EELNES spectra in complex oxides. The present calculation underscores the importance of not only including the electron-hole interaction, but also the transition matrix elements, and to a certain extent, the difference in the transition energies from different sites.

In the so-called low-loss region, the energy-loss spectra can be obtained from the complex frequency-dependent dielectric function. The traditional approach for the calculation of the dielectric function of insulators is along the line of the interband optical transition.[16] Such calculations can usually provide good agreement with the measured optical data.[22–24] However, significant disagreement can result in some cases, especially near the absorption edge. Apart from the well-known problem of gap underestimation associated with the deficiency in the local-density approximation (LDA) theory, a particular drawback in the interband optical calculation is its inability to reproduce the excitonic features near the VB absorption edge. In α-Al_2O_3, Y_2O_3, and α-quartz, the presence of the prominent excitonic feature in the optical spectra is quite clear.[17–20] In YAG, the excitonic feature is less prominent.[7] We have calculated the optical properties of YAG by including the VB exciton. To account for the more delocalized nature of the VB exciton, we have used the 160-atom full cubic cell. Since the cell is sufficiently large, only one general *k* point is used for Brillouin-zone integration. The computational procedure is similar to the EELNES calculation, except that in this case, a final state is obtained in which an electron at the top of the VB is excited to the lowest CB. The initial states are the VB states from the ground-state calculation. The interaction between the electron-hole pair is again accounted for by the self-consistent iterations for the final state. The imaginary part of the dielectric function, $\varepsilon_2(\hbar\omega)$, is obtained first from interband transitions. The real part of the dielectric function, $\varepsilon_1(\hbar\omega)$, is obtained from $\varepsilon_2(\hbar\omega)$ by the Kramers-Kronig conversion. The resulting complex dielectric function is displayed in Fig. 4(b), which is to be compared with the measured data by Tomiki *et al.*[7] reproduced in Fig. 4(a). The agreement in the peak structures, shapes, and relative intensity between the two is very good. The static dielectric constant (the electronic part of the dielectric function at zero frequency) $\varepsilon_0=\varepsilon_1(0)$ of 3.54 is in good agreement with Tomiki's value of about 3.4. The onset of absorption, which

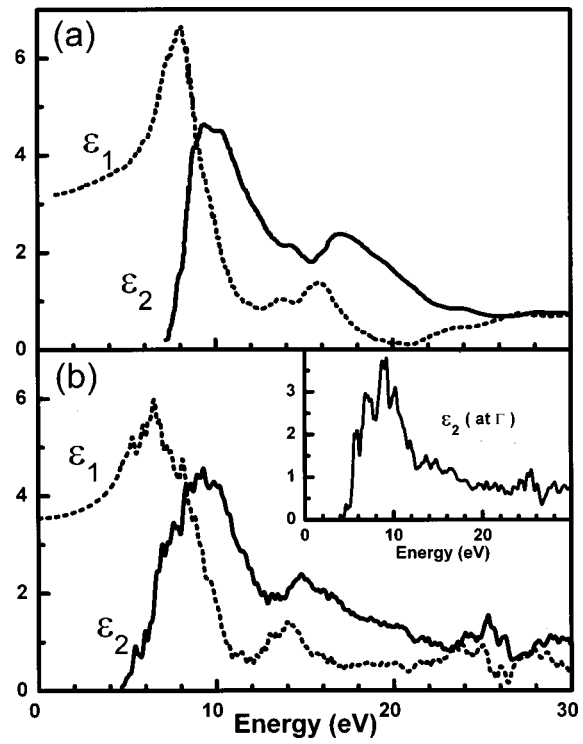

FIG. 4. (a) Experimental real and imaginary parts of the dielectric function (Ref. 11). (b) Results from the present calculation. The inset shows the $\varepsilon_2(\hbar\omega)$ from the Γ point.

defines the optical band gap, is underestimated by about 30%. However, a rigid shift of the CB (scissors operator) will not be valid, since the position of the main peak in $\varepsilon_2(\hbar\omega)$ at around 9.5 eV is already in close agreement. Clearly, an improved agreement in the VB optical spectrum of YAG will require a theory for excited states beyond the LDA theory. Another source of disagreement could be due to the fact that the YAG sample used in the experiment may contain traces of impurities such as Nd or Ce. Tomiki *et al.* had pointed out that the weak feature near the absorption onset at 7.0 eV is due to the VB exciton.[11] This feature is actually reproduced in our calculation, and can be more easily identified from the calculation done at the Γ point, which is shown in the inset of Fig. 4. The lowest CB of YAG is at Γ and any excitonic effect should be more pronounced at the zone center. In α-Al_2O_3, the same excitonic effect produces a sharp peak near the absorption edge.[18] Our preliminary VB exciton calculation on α-Al_2O_3 has reproduced this sharp feature.[25] The reason for the much weaker exciton feature in YAG is not clear. It is possible that the excitonic feature is somehow located within the bulk CB. Inspection of the plot of $|\psi_\Gamma|^2$, where ψ_Γ is the wave function of the lowest CB at Γ on the (001) plane, reveals this state to be quite delocalized. We have also investigated the excitonic effect in which the excited electron originates from the semicore Y 4*p* state and from the deep O 2*s* band, instead of from the top of the VB. In each case, we find the changes in the optical spectra to be negligible. This suggests that the main excitonic feature in YAG should be from the top of the VB.

In conclusion, we have presented a calculation of the op-

tical spectra in a YAG crystal by a state-of-the-art method that accounts for the excitonic effect in the core-level and VB transitions. It is clearly shown that the excitonic effect cannot be neglected, especially in the core-level transitions, and must be part of any spectroscopic interpretation in insulators. The site-specific EELNES spectral calculation can be extremely valuable in the structural characterization of microstructures and microdefects in complex ceramic materials.

This research was supported by the U.S. Department of Energy under Grant No. DE-FG02-84DR45170 and the NEDO international grant.

*Author to whom all correspondence should be addressed. Email address: chingw@unkc.edu

[1] G. deWith, in *High Technology Ceramics*, edited by P. Vincenzini (Elsevier, Amsterdam, 1987), p. 2063.
[2] R. C. Powell, in *Physics of Solid State Laser Materials* (AIP, New York, 1998).
[3] F. Euler and J. A. Bruce, Acta Crystallogr. **19**, 971 (1965).
[4] Y.-N. Xu and W. Y. Ching, Phys. Rev. B **59**, 10 530 (1999); W. Y. Ching and Y.-N. Xu, *ibid.* **59**, 12 815 (1999).
[5] W. L. Bond, J. Appl. Phys. **36**, 1674 (1965); G. A. Slack, D. W. Oliver, R. M. Chrenko, and S. Roberts, Phys. Rev. **177**, 1308 (1969); N. S. Rooze and N. A. Anisilmov, Trudy Inst. Fiz. Akad. Nank. Est SSR **44**, 163 (1975).
[6] T. Tomiki, F. Fukudome, M. Kaminao, M. Fujisawa, Y. Tanahara, and T. Futemma, J. Phys. Soc. Jpn. **54**, 4429 (1988); **58**, 1801 (1989).
[7] T. Tomiki, Y. Ganaha, T. Shikenbrau, T. Futemma, M. Yuri, Y. Aiura, H. Fukutani, H. Kato, J. Tamashiro, T. Miyahara, and A. Yonesu, J. Phys. Soc. Jpn. **62**, 1388 (1993); **65**, 1106 (1996).
[8] J. D. French, J. Zhao, M. P. Harmer, H. M. Chan, and G. A. Miller, J. Am. Ceram. Soc. **77**, 2857 (1994).
[9] S. Deng, Mater. Sci. **31**, 6077 (1996); R. S. Hay, J. Am. Ceram. Soc. **77**, 473 (1994).
[10] G. S. Gorman, Report No. USAF/WRPC-TR-90-4059, 1990 (unpublished).
[11] C. M. Wang, G. S. Cargill, M. P. Harmer, H. M. Chan, and J. Cho, Acta Mater. **47**, 3411 (1999).
[12] R. F. Egerton, *Electron Energy Loss Spectroscopy in the Electron Microscope* (Plenum, New York, 1996).
[13] M. A. Gülgün, W. Y. Ching, Y.-N. Xu, and M. Rühle, Philos. Mag. B **79**, 921 (1999).
[14] I. Tanaka, J. Kawai, and H. Adachi, Phys. Rev. B **52**, 11 733 (1995).
[15] A. J. Scott, R. Brydson, M. MacKenzie, and A. J. Craven, Phys. Rev. B **63**, 245105 (2001).
[16] H. Raether, *Excitations of Plasmons and Interband Transitions by Electrons*, Springer Tracts in Modern Physics Vol. 88 (Springer-Verlag, Berlin, 1979), p. 9.
[17] E. T. Arakawa and M. W. Williams, J. Phys. Chem. Solids **29**, 735 (1968); T. Tomoki, T. Futemma, H. Kato, T. Miyahara, and Y. Aiura, J. Phys. Soc. Jpn. **58**, 1486 (1989).
[18] M. L. Bortz, R. H. French, D. J. Jones, R. V. Kasowski, and F. S. Ohuchi, Phys. Scr. **41**, 4404 (1990); M. L. Bortz and R. H. French, Appl. Phys. Lett. **55**, 1955 (1989).
[19] V. N. Abramov and A. I. Kuznetsov, Sov. Phys. Solid State **20**, 399 (1978); Tomiki *et al.*, J. Phys. Soc. Jpn. **61**, 2961 (1992).
[20] C. Tarrio and S. E. Schnatterly, J. Opt. Soc. Am. B **10**, 952 (1993).
[21] S. D. Mo and W. Y. Ching, Phys. Rev. B **62**, 7901 (2000).
[22] W. Y. Ching and Y.-N. Xu, Phys. Rev. Lett. **65**, 895 (1990); Y.-N. Xu, Z.-Q. Gu, and W. Y. Ching, Phys. Rev. B **56**, 14 993 (1997).
[23] W. Y. Ching and Y.-N. Xu, J. Am. Ceram. Soc. **77**, 404 (1994).
[24] W. Y. Ching, Z.-Q. Gu, and Y.-N. Xu, Phys. Rev. B **50**, 1992 (1994).
[25] Y.-N. Xu and W. Y. Ching (unpublished).